Resonant infrared two-photon ionization of D($n=8$) atoms

J. E. Bayfield and D. W. Sokol
Department of Physics and Astronomy, University of Pittsburgh, Pittsburgh, Pennsylvania 15260
(Received 14 April 1986)

Two-photon ionization of hydrogenic atoms with principal quantum number $n=8$ has been studied experimentally over the wavelength range 10.45—10.59 μm. The ionization was resonantly enhanced by the $n=12$ intermediate state, with a large $n=8$ to $n=12$ coupling responsible for a fractional resonance width of about 0.1%. On resonance, ionization rates of order 10 MHz were achieved with nominal 2-mJ, 40-nsec laser pulses, with 40 mJ being required at wavelengths 1% away from resonance. The data are interpreted in terms of the extended two-level model for multiphoton ionization. The peak laser electric field strength reached values where the top of the instantaneous potential energy barrier was near the intermediate-state energy value.

I. INTRODUCTION

The lower highly excited states of atoms and molecules can be ionized by the absorption of a few quanta of infrared radiation at wavelengths in the 9—11 μm region of operation of carbon dioxide gas lasers. In the hydrogenic atom, the levels energetically open for two-photon ionization have principal quantum number of values of $n=8$, 9, and 10. Some typical transitions are shown in Fig. 1. The $n=7$ level can be ionized by the absorption of three quanta ($k=3$), while the $n=6$ level requires four quanta.

Theoretical predictions of the multiphoton ionization rates for such processes have been restricted to perturbative calculations for the two-photon ionization of excited hydrogen atoms with known principal quantum number, with an average being taken over the remaining quantum numbers of the atom.[1,2] Within the realm of conventional perturbation theory, a quantum calculation that exactly includes all intermediate states was reported by Justum and Maquet, who utilized a pseudostate approach to both eliminate the continuum contribution and to make the summation over the infinite bound states tractible.[1] A perturbative quasiclassical calculation by Berson has produced an analytical result that is in excellent agreement with the perturbative quantum results.[2] In the fast-atom-beam experiments to be described, atoms were present in the beam with a distribution of principal quantum numbers. Assuming this distribution were to be uniform, Berson's formula would predict the wavelength dependence of our overall two-photon ionization signals from the summed two-photon ionization cross section shown in Fig. 2. The resonance contributions from $n=8$, 9, and 10 appear at different wavelengths. For cross-section values above 10^{-24} cm^4/W, which produce observable ionization for laser-pulse energies less than 100 mJ in our experiments, the $n=8$ signal is expected to dominate at most wavelengths between 10.45 and 10.59 μm, both because of unusually large matrix elements for the bound-bound first transition to an unusually low-lying intermediate state, and because of an unusually large and near-threshold intermediate-state photoionization cross section.

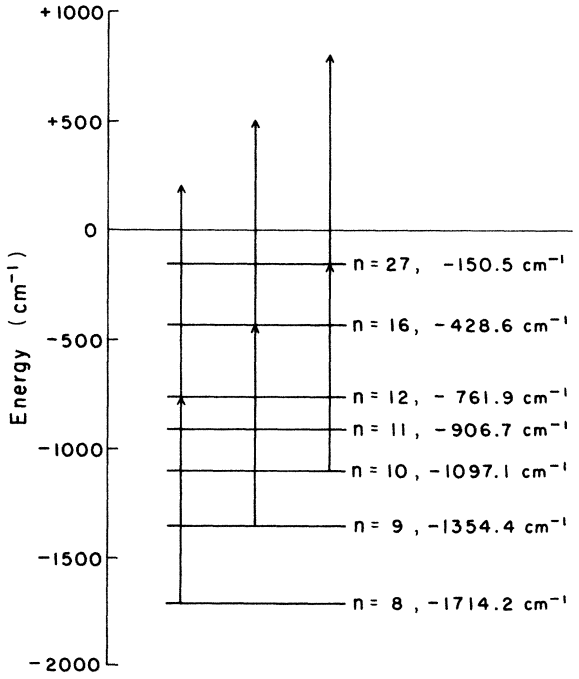

FIG. 1. An energy-level diagram of some excited-state energy levels of the hydrogen atom, indicating some typical resonant two-photon ionization processes that can occur in the wavelength region 9—11 μm.

The theoretical curves of Fig. 2 are inaccurate, primarily in that unmodified perturbation theory does not yield the widths and shifts of the resonances; the near-resonance ionization cross section is grossly overestimated and incorrectly becomes infinite on resonance. Although general theory has been developed for the corrections to two-photon ionization perturbation theory that provide values for the laser-intensity-dependent widths and shifts,[3] it has not yet been applied to the present problem. We therefore shall use the nonperturbative extended two-level semiempirical model[4] in analyzing and interpreting our experimental results. This model describes the two-photon ionization in terms of a Lorentzian resonance formula that contains dependences on the individual rates for the bound-bound and bound-continuum one-photon steps for the overall ionization process, and includes laser band-

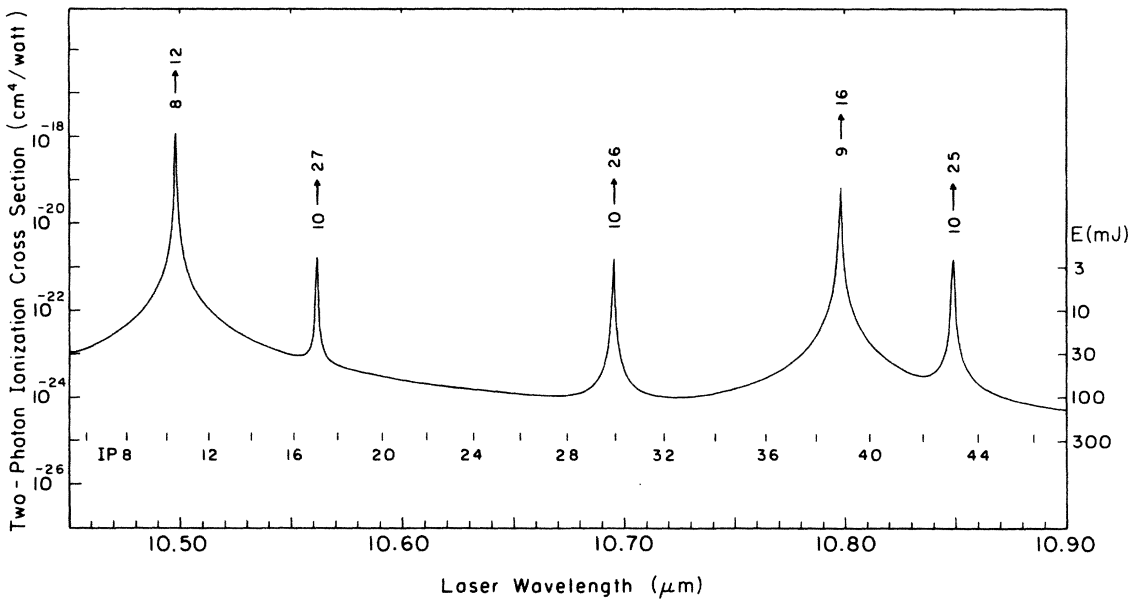

FIG. 2. Perturbative quasiclassical predictions for the two-photon ionization cross section summed with equal weights over the $n=8-10$ range of states present in the atomic beam. Approximate 40 nsec laser pulse energies for 60% ionization probability are indicated on the right hand scale.

width modifications to approximately account for a nonmonochromatic laser field. This does not account properly for the multimode characteristics of the laser beam used in our experiments, although such effects on the resonance rate, width, and frequency shift are expected to be relatively small for the low-order two-photon ionization case.[5,6]

The only reported experimental observation of apparent CO_2-laser two-photon ionization of excited atomic states was the reduction in strength of Balmer emission lines from a hydrogen discharge when exposed to laser radiation at a single wavelength.[7] This was noticed during a study of the laser-induced optical Stark shifts of those Balmer lines, undertaken for a first rough comparison with the perturbative predictions for the laser-induced quasienergy state spectrum made by several investigators.[8–11] We also shall be concerned with the question of optical Stark shifts of the two-photon ionization resonance wavelength value; these may be estimated by the quasienergy-state spectral line shifts, but, in general, the two types of shifts are not expected to be the same.[3] In particular, uncorrected perturbation-theory values for the shifts are not expected to apply at wavelengths near intermediate-state resonances.

II. DESCRIPTION OF THE EXPERIMENTS

Our experimental technique utilized collinear pulsed TEA CO_2 laser and fast-excited-deuterium-atom beams, with the laser wavelength being tuned both by changing the laser line and by changing the atom velocity to vary the Doppler effect.[12] Figure 3 shows a schematic diagram of the apparatus, which contains as principal components (1) a 5–30-keV deuteron beam source and accelerator, (2) a freon-gas charge exchange scattering cell for collisionally transferring electrons from freon molecules to the fast deuterons passing through, (3) a pulsed-CO_2-laser oscillator amplifier system that produces an unfocused infrared light beam propagating collinear and opposite to the fast-deuterium-atom beam, (4) a magnet for selecting the photoionization product fast deuterons and directing them into a particle multiplier, and (5) a computer-controlled electronic data-acquisition system for measurement of the product deuteron count rates on a laser shot-by-shot basis first for the laser light off and then after exposure to the laser pulse.

The deuteron ion beam source and accelerator was a High Voltage Engineering Corp. model CN Van de Graaff accelerator with the usual radio-frequency gas discharge ion source, but with the terminal charging system normally used to provide the high voltage replaced by a voltage-regulated high-voltage power supply. This system regularly delivered several microamperes of deuterons through the charge exchange cell, as determined by a translatable Faraday cup that could be moved into the beam at a location just before the second ion magnetic analyzer, see Fig. 3. The ion beam was effectively collimated by two apertures 1 cm in diameter separated by 1.2 m. The choice of deuterons rather than protons was predicated by the need for slower atom velocities, which enabled us to time-separate the laser photoionization product pulses coming from the particle detector from electrical noise pulses associated with the firing of the laser pulse amplifier. The H_2^+ contamination of the deuteron beam was assessed both from the levels of H^+ and H_3^+ ions coming from the accelerator and from the level of dissociation product H^+ produced with argon gas in the charge exchange cell; the H_2^+ contamination was

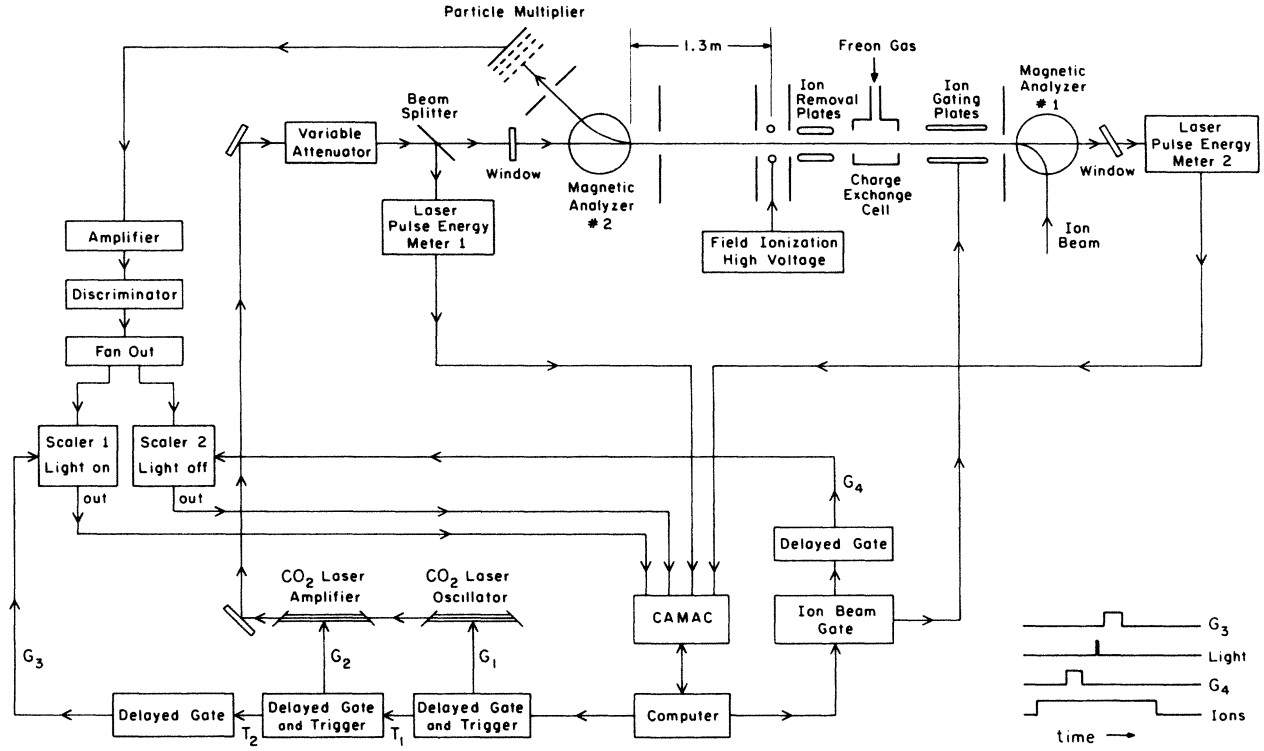

FIG. 3. Schematic diagram of the apparatus built for the study of pulsed CO_2-laser interactions with excited atoms in a fast atomic beam.

normally at most 0.4%. Any charged dissociation products originating from H_2^+ were rejected by the second ion analyzer magnet located before the particle multiplier. Thus the small level of H_2^+ contamination in the ion beam did not directly create any background ion count rates related to the presence of the laser pulse. Laser photoionization of 1% of the total neutral H_2 molecular beam produced by charge transfer of the contaminant H_2^+ beam would have been observed at the background noise level of our experiments.

The production by charge exchange of fast deuteron beams adequately excited into the $n=8$ state was achieved using both argon- and freon-gas targets. More is known about the cross sections involved for the argon case,[13] while freon[14] produced a 50% larger excited-state fraction. In both cases the gas pressure was set for about 15% total charge exchange probability for the incident deuteron beam. The charge exchange cell was pumped by a 9-in. liquid-nitrogen-trapped diffusion pump, and the apparatus on either side of the charge exchange region was further differentially pumped by three 6-in. trapped diffusion pumps. The pressure in the 1.3-m laser-beam—atom-beam interaction region, see Fig. 3, was 2×10^{-7} Torr during the acquisition of data.

Before entering the charge exchange cell, the ion beam was chopped with a 0.1% duty factor by a gated transverse electric field between the gating plates of Fig. 3. This was to reduce the time-average particle multiplier output current, enabling it to be operated at higher voltage and thereby at higher gain. A second pair of transverse electric field plates after the charge exchange cell removed all ions from the fast beam at that point. A pair of parallel metal rods located just before the beam-beam interaction region was operated at a peak electric field strength of about 47 kV/cm and field-ionized most atoms in the beam with principal quantum numbers larger than 10.[15] This reduced the background ion count rate arising from laser one-photon ionization of these atoms from 4 times the two-photon ion count rate to at most 7% of that rate. The background ion count rate due to fast-atom stripping in the residual gas in the interaction region was about equal to the maximum two-photon ionization count rate, and was measured with the laser pulse absent.

The CO_2 laser oscillator was a standard Tachisto TAC IIG grating-tuned TEA laser, while the laser amplifier was a Lumonics model No. 203 three-stage device operated in single-pass mode at a pulse-energy gain of about 10. The oscillator internal aperture was set at a small enough diameter to produce a TEM_{00} transverse output mode as observed on a graphite target. However, the oscillator laser pulse was not single longitudinal mode, resulting in mode beating in the pulse temporal development and a relatively large laser effective bandwidth.[16] The relative timing of the trigger pulses for the oscillator and amplifier was adjusted to maximize the final laser-beam pulse energy. The oscillator gas pressures were set at values that resulted in a large gain-switched initial spike in the laser output pulse, as observed using a photon drag detector and an oscilloscope. About half the pulse energy was in this initial spike. The total laser pulse energy for the laser beam entering the evacuated fast-atom-beam apparatus was sampled by a calibrated laser-beam splitter

and measured by a first laser pulse-energy meter, Laser Precision model No. RK3230. The laser pulse-energy transmitted through the entire apparatus was monitored by a second pulse-energy meter, so that the laser-beam transmission could be assessed on a shot-by-shot basis. Data acquired during "bad" shots, having low pulse energy or low transmission, could be automatically rejected in real time by the data-acquisition computer. The maximum available laser pulse energy in the atomic-beam interaction region varied with laser line, but often reached 40 mJ. The actual laser pulse energy used in each experimental run was adjusted by a II-VI Company model No. PAZ-20-WC crossed-polarizer CO_2-laser-beam variable attenuator. The attenuator was placed in the beam in a manner that assured fixed laser-beam polarization for the beam entering the interaction region.

The particle multiplier was a Johnston model MM I. It was operated with a 300-Ω resistor between anode and grounded backplate, and was ac coupled into a 100-MHz integrated-circuit pulse amplifier-discriminator, LeCroy type No. MVL-100, operated with an output pulse width of 20 nsec. It was established by experiments varying the atom beam intensity and using the full laser one-photon background photoionization signal that the entire ion pulse detection system was linear within 10% up to peak ion counting rates of 5 counts per shot. Since each shot produced a 1.3-m-long "slug" of fast ions traveling toward the detector at a speed of about 10^{+8} cm/sec, this peak counting rate corresponded to instantaneous counting rates of about 5 MHz.

The control of the experiment, including data acquisition and system monitoring on a shot-by-shot basis, was in the hands of a Kinetics Systems model No. 8030 CAMAC system containing a local 8-bit microcomputer system capable of addressing digital-analog and analog-digital converter, 100 MHz scalar and pulse generator modules via programs written in BASIC code. A sequence of LeCroy type No. 222 delayed gate generator module pulses was triggered by a computer-generated initial fast trigger pulse. The gate generators produced the sequence of timed events sketched in the lower right corner of Fig. 3. First the deuteron beam was gated on for a 1.5-msec interval. In the middle of this interval, pulse counting scalar No. 2 was gated on for a 0.90-μsec interval to obtain a measure of the background count rate, i.e., with no laser light present. About 20 μsec later, appropriately timed trigger pulses were sent to the laser oscillator and amplifier, which in turn produced the laser pulse after a time delay. The resultant ions reached the particle detector and produced ion pulses after a further time delay. At an appropriate point in time, a second gate pulse of duration equal to that for the scalar No. 2 gate time was used to gate scalar No. 1 and obtain a measure of the total ion count rate with the laser light present. Using the full photoionization background signal, data was taken as a function of the time delay of the scalar No. 1 gate pulse, to assure that this scalar accumulated counts generated only while the laser light was present.

A typical data point was taken at fixed laser wavelength and atom beam energy, with the laser shots being fired at a 0.5-Hz rate over a period of up to 1 h. The computer accumulated light-on counts, light-off counts and laser pulse-energy values on a shot-by-shot basis, and calculated total difference signals normalized to the total light-off signal, along with statistical errors for this normalized signal and for the average laser pulse energy. Typically 1 to 3 counts would be accumulated per laser shot. A successful day-long run would involve taking perhaps ten data points at different laser pulse energies, and thirty such runs were taken over eleven different Doppler-tuned laser frequencies.

III. EXPERIMENTAL RESULTS AND ANALYSIS

Run-averaged experimental data for the dependence upon laser pulse energy of the ion-count-rate ratio defined just above are shown in Fig. 4 for two different wavelengths. The two-photon ionization signal clearly varies with laser wavelength, unlike that observed for the one-photon $n > 10$ background signal. The residual apparent signal at low laser pulse energies is due to a combination of residual one-photon ionization and residual scalar gate-time asymmetry. At high laser pulse energies the ion-count-rate ratio experimentally saturates when all the $n = 8$ atoms present in the apparatus during the laser pulse are ionized.

A preliminary determination of the laser-wavelength dependence of the two-photon ionization was made by plotting the values for the 60% probability points in the ion-count-rate ratio signals of the type shown in Fig. 4. The data points with error bars in Fig. 5 are the results. A resonant minimum in the laser pulse energy needed for 60% ionization probability is found to lie close to the expected $n = 8$ to $n = 12$ resonance wavelength of 10.500 μm. The large error bars for the data points at 10.533 and 10.553 microns arose from some irreproducibility in the data from month to month. That these wavelengths

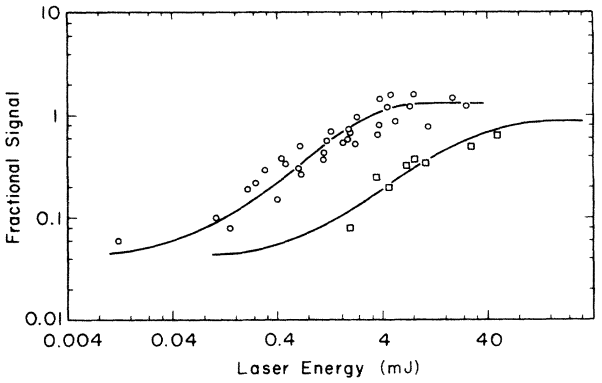

FIG. 4. The variation of the two-photon ionization fractional signal with laser pulse energy, near resonance (10.491 μm) and in the resonance wings (10.591 μm). At lower pulse energies a small one-photon ionization background remains, while at high pulse energies the two-photon ionization signal experimentally saturates. The solid curves are results of a fit to all the data at all the wavelengths investigated.

are near the 10.564 μm wavelength for the $n=10$ to $n=27$ resonance shown in Fig. 2 may or may not be coincidental.

Our procedure for analyzing the data next involved a trial-by-error fit to the extended two-level (ETL) model formula,[4] using reasonable values for the physical parameters that enter. The formula for the dependence upon laser intensity I of the ion-count-rate ratio $f(I)$ can be written as

$$f(I)=b_1+b_2\left[1-\exp\left[-\frac{\frac{1}{4}\Omega_R^2(R_{2c}+\Gamma)\Delta t}{(\Delta\omega-sI)^2+\frac{1}{4}(R_{2c}+\Gamma)^2+\frac{1}{2}\Omega_R^2(1+\Gamma/R_{2c})}\right]\right], \tag{1}$$

where Ω_R is the bound-bound Rabi-flopping transition rate, R_{2c} is the bound-continuum transition rate, Γ is the laser bandwidth, sI is the optical Stark shift of the resonance frequency, $\Delta\omega$ is the frequency deviation from the unshifted resonance, $\Delta t=40$ nsec is the effective time duration of the laser pulse, and the constants b_1 and b_1+b_2 are the asymptotic values of the function $f(I)$ at small and large values of I, respectively. The quantity Ω_R is proportional to the off-diagonal coupling matrix element between the $n=8$ and $n=12$ states, and to the square root of the laser intensity. The matrix elements for different possible quantum numbers n, l, m can be found in Ref. 17. The quantity R_{2c} is proportional to the $(n=12)$-state photoionization cross section and to the laser intensity. Exact values for the cross sections for different possible quantum numbers can be evaluated using the formulas in Ref. 18. The optical shift sI is approximately proportional to the difference in the wavelength-dependent optical polarizabilities of the $n=8$ and $n=12$ states, and to the laser intensity. It also depends upon all the quantum numbers.[10] If the optical shifts for our ionization-resonance data points were comparable to that observed for the Balmer α lines,[7] they could be as large as 100 MHz/mJ. We define parameter coefficients a_1, a_2, and s_1 by the expressions

$$\Omega_R(I)\equiv a_1E^{1/2}, \tag{2}$$

$$R_{2c}(I)\equiv a_2E, \tag{3}$$

$$sI\equiv s_1E, \tag{4}$$

where the laser intensity I is related to the laser-pulse total energy E in mJ by $I=E/A\Delta t$, and $A=2.5$ cm^2 is the nominal cross-sectional area of the aperture-collimated laser beam.

There is insufficient information about the substate population of excited-state beams produced by charge exchange for us to determine the contributions to our two-photon ionization signal from the different types of $n=8$ atoms. The $8p$ and $8d$ populations are significantly depleted by optical decay after the field-ionization region; on the other hand, the motional electric field produced by the atoms moving in the earth's magnetic field and the strength of the laser electric field are both large enough for a description of the $n=8$ states in terms of the spherical quantum numbers to be questionable. Thus we will model our data to single substate-averaged values for the parameters a_1 and a_2. The ranges of expected values are a_1 between 0.54 and 15 GHz/mJ$^{1/2}$ and a_2 between 28 and 62 MHz/mJ.

We carried out a computer least-squares fitting of the ETL model Eq. (1) to the data, using the CERN general purpose nonlinear multiparameter fitting routine MINUIT.[19] The best procedure was found to be a division of the fitting problem based upon the nature of the ionization near resonance and in the resonance wings. Near resonance, where $\Delta\omega-sI\ll\Omega_R(1+\Gamma/R_{2c})^{1/2}$, Eq. (1) becomes

$$f'(E)=b_1+b_2\left[1-\exp\left[-\frac{R_{2c}\Delta t}{2}\right]\right], \tag{5}$$

which physically arises because the bound-bound transition saturates while dominating the denominator in Eq. (1). The near-resonance data then directly determines a_2. Using this value of a_2, the data in the wings is fit to the full ETL formula, varying a_1, Δt, and Γ. In the far off-resonance limit we note that Eq. (1) becomes

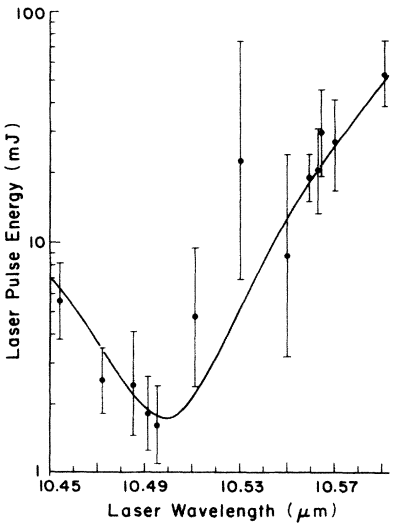

FIG. 5. The variation with laser wavelength of the laser pulse energy required for 60% two-photon ionization of $n=8$ deuterium atoms. The data points are averaged values for several experimental runs, with error bars indicating the largest observed variations. The curve is a fit to the ETL model.

$$f''(E)=b_1+b_2\left[1-\exp\left[-\frac{\Omega_R^2(R_{2c}+\Gamma)\Delta t}{(\Delta\omega)^2}\right]\right]. \quad (6)$$

If the bound-continuum rate R_{2c} is small compared to the laser bandwidth Γ, this expression does not depend upon the former. We thus note that under the above circumstances the dependence of the two-photon ionization rate on laser intensity is nearly linear both near resonance and in the far wings, for different reasons. This explains the similarity of the two curves in Fig. 4, neither being quadratic in their behavior at the lower laser pulse energies of the beginning of the steps, after background subtraction.

Results based upon our computer runs were the values $a_1=6.6\pm2$ GHz/mJ$^{1/2}$, $a_2=24\pm5$ MHz/mJ, $s_1=3\pm1$ GHz/mJ, and $\Gamma=5\pm2$ GHz. Here the error bars represent changes that produced noticeably worse fits. The values obtained for a_1, a_2, and Γ are within the expected range of values for these parameters, while s_1 is unexpectedly large. Figure 6 compares the ETL two-photon cross section calculated for these values, except for setting $s_1=0$, with two other cross sections, one of the ETL cross section with the nonperturbative width terms neglected and the other the exact perturbative curve given by the quasiclassical formula.[2] The experimental results are in satisfactory agreement with these theoretical expectations.

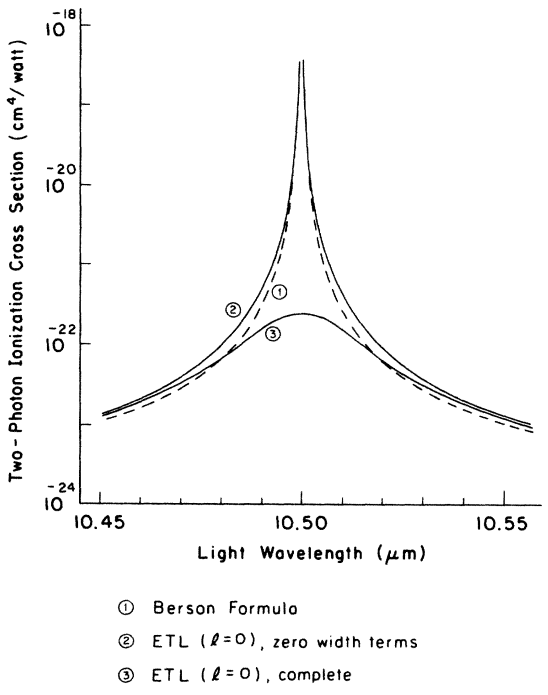

FIG. 6. Comparison of the perturbative quasiclassical two-photon ionization cross section for $n=8$ with ETL model predictions without resonance width terms, curve 2, and with experimentally-determined width terms, curve 3. Both laser power broadening and laser bandwidth contribute to the resonance width for curve 3.

The observed optical Stark shift parameter value 3 GHz/mJ is 30 times expected values. We have no good explanation for this. The calibration of our Optical Engineering CO_2 laser spectrum analyzer was checked during studies with another apparatus that used high-resolution cw CO_2 laser excitation of state-selected highly excited hydrogen atoms.[20,21] Thus there seems no possibility of misidentification of laser lines, which would create wavelength-measurement errors. A possible explanation to be investigated theoretically is the optical induction of a first-order dipole moment in the atom.

IV. DISCUSSION

The primary motivation for the present experiments was to search for anomalous ionization of the $n=12$ intermediate state. The present work follows a sequence of multiphoton ionization experiments that have not been explained by the usual perturbative picture of photoionization that is based upon one or more steps of photon absorption involving off-diagonal electric-dipole radiative coupling matrix elements between field-free atomic states. These experiments are of two types, (a) those requiring enormous numbers of photons to be absorbed in order for the free-atom ionization limit to be energetically reached, and (b) those with energetically allowed one-photon ionization, but exhibiting ionization that behaves very differently from usual single-photon ionization. The first type includes the microwave ionization of highly excited hydrogen atoms[20,21] and the CO_2 laser ionization of xenon and krypton atoms.[22] The second type was observed in the anomalous ionization of the $n=10$–20 Ry states of the sodium atom by a 1.06 μm laser field.[35] These experimental observations are all evidence for a strong-field ionization enhancement mechanism that arises from a dynamic distortion of the atomic potential, accompanied by a polarization of the atom. Ionization then proceeds via this distortion as a high-order electric dipole interaction with the radiation field that partially manifests itself through diagonal matrix elements for the distorted atom, its states being of mixed parity.

Let us take as a hypothesis that these anomalous ionization processes occur because on time average a portion of the ionization energy is absorbed by the atomic electron during one peak half-period of each oscillation of the radiation field. This period is half the time, when the peak field strength is about 20% higher than that needed for the barrier in the peak instantaneous potential to be down to the energy of the bound state of interest. We can then make a classical estimate of the conditions needed for complete ionization after N oscillations of the field. A rough scaling law will be the result, with all the anomalous data being consistent with it within 2 orders of magnitude.

Let us begin by assuming that the electron is partially free from the nuclear Coulomb field during the time interval δt when the barrier is below the energy of the initial atomic state. Then Newton's law yields an approximate electron acceleration $(eF/m)\cos(\omega t)$, where F is the peak laser field strength and ω is the laser angular frequency. If the electron is to have left the atomic nucleus after N

field oscillations, then classically it must net gain $1/N$ of the original binding energy E_n during each cycle of the field. Setting this fractional acquired energy to be at least equal to the work done by the field on the electron during the duration of the barrier height minimum of about $\frac{1}{4}$ a field oscillation (in atomic units)

$$\frac{E_n}{N}=\frac{1}{N}\left[\frac{1}{2n^2}\right]\leq\int_{\delta t}F(t)v(t)dt$$
$$=\frac{F^2}{\omega}\int_{-\pi/4\omega}^{\pi/4\omega}\sin(\omega t)\cos(\omega t)dt=\frac{F^2}{2\omega^2}\ , \tag{7}$$

where $E_n=1/(2n^2)$ defines n. We deduce that ionization enhancement will not occur unless

$$\frac{\omega}{nF}\leq N^{1/2}\ . \tag{8}$$

The classical condition that the peak barrier be below the initial energy is[24]

$$F\geq F_c\equiv(16n^4)^{-1}\ . \tag{9}$$

Inequalities (8) and (9) are equivalent to the single inequality

$$F^2/\omega\geq(16n^5N^{1/2})^{-1}=2^{-3/2}N^{-1/2}E_n^{5/2}\ , \tag{10}$$

or changing away from atomic units

$$I\ (\text{in W/cm}^2)\times\lambda\ (\text{in mm})\geq 9\times10^8N^{-1/2}[E_n(\text{eV})]^{5/2}\ , \tag{11}$$

a relation between the laser-intensity laser-wavelength product and the binding energy of the atomic state E_n. Table I lists values for the experiments mentioned above, as well as for the present experiment. For the last two listed cases of one-photon ionization, we account roughly for the quantum inhibition of classical behavior,[25] by taking $N=1$; the photon then must be absorbed during one particular field oscillation. While the earlier experiments observing anomalous ionization obey Eq. (10), the present one does not, although the peak field strength is at least close to sufficient to pull the barrier down below the binding energy level, see Table I. We point out that if our experiment were repeated with the high-power picosecond CO_2-laser pulses now available,[26] then the peak field for significant ionization would be 100 times the present value and we would have $F\gg F_c$.

It is of interest to further discuss the possibility of multiphoton ionization of the atoms in our atomic beam that possessed principal quantum numbers other than 8. Estimates of this can be carried out using the multiphoton generalizations of the quantities Ω_R and R_{2c} in the ETL model.[27] In analogy with the situation for high-order microwave absorption of very highly-excited hydrogen atoms,[21] we assume that the photon absorption develops as much as possible via the oscillating Stark effect, i.e., via large diagonal matrix elements for the mixed-parity states produced by the optical Stark mixing by the laser field. There must be one off-diagonal matrix element cou-

TABLE I. Comparison of characteristic parameters for experimental anomalous photon ionization of atoms at high intensities I, different degrees of atom electron binding parameter n, and different field wavelengths λ. The parameters are defined in the text. The column labeled $I\lambda$ is to be compared with the last column; only for the present experiment is the $I\lambda$ value the smaller.

Ref.	n	λ (mm)	F (V/cm)	F_c (V/cm)	I (W/cm)	$I\lambda$	N	E_n (eV)	$9\times10^8N^{-1/2}E_n^{5/2}$
20,21	63	40	12	20	0.2	8	3×10^3	0.003	8
22	1	0.0096	1.7×10^8	3.2×10^8	4×10^{13}	3.8×10^{11}	3×10^4	12.1	2.7×10^9
32	1	1.9×10^{-4}	2.7×10^8	3.2×10^8	10^{14}	1.9×10^{10}	1.6×10^4	12.1	3.7×10^9
23	17	0.001	6.4×10^5	3.8×10^3	5×10^8	5×10^5	1	0.05	5×10^5
23	26	0.001	6.4×10^5	700	5×10^8	5×10^5	1	0.02	5×10^4
This work	12	0.01	1.4×10^4	1.5×10^4	2.5×10^5	2.5×10^3	1	0.09	2×10^6

pling the initial and intermediate bound states, and another coupling the intermediate state with a continuum state. For example, consider the bound-bound Rabi transition rate Ω_R in a two-state approximation. Each state is an oscillating Stark orbital involving the diagonal matrix element $z_{nn}=(\frac{3}{2})n(n_1-n_2)F$:[24,28,29]

$$\psi_n(\mathbf{r},t)=\phi_n(\mathbf{r})\exp\left[-iE_nt-i\frac{z_{nn}F}{\omega}\sin(\omega t)\right], \tag{12}$$

$$\psi_n(\mathbf{r},t)=\phi_n(\mathbf{r})\exp(-iE_nt)\sum_{k=-\infty}^{\infty}J_k(z_{nn}F/\omega)e^{-ik\omega t}. \tag{13}$$

To first order in the off-diagonal coupling $z_{n'n}F$, the perturbative transition amplitude for the state n' is

$$a_{n'}(t)=\int\psi_{n'}^{*}[zFe^{-i\omega t}]\psi_n d^3r\,dt \tag{14}$$

$$=z_{n'n}F\sum_{k=-\infty}^{\infty}\sum_{k'=-\infty}^{\infty}J_k(z_{nn}F/\omega)J_{k'}(z_{n'n'}F/\omega)\int^{t}e^{-i(k-k'+1)\omega t}e^{-i(E_n-E_{n'})t}dt, \tag{15}$$

where as usual the only terms having large nontransient values for the time integral are the energy-conserving ones with $(k-k'+1)\omega=E_{n'}-E_n\equiv\alpha\omega$. The double sum thus becomes a single sum, and the coefficient of the time-dependent factor is the multiphoton Rabi moment

$$M_{n'n}=z_{n'n}F\sum_{k=-\infty}^{\infty}J_k(z_{nn}F/\omega)J_{k-(\alpha-1)}(z_{n'n'}F/\omega). \tag{16}$$

The final summation can be performed using the addition theorem for Bessel functions to yield

$$M_{n'n}=z_{n'n}FJ_{\alpha-1}((z_{nn}-z_{n'n'})F/\omega). \tag{17}$$

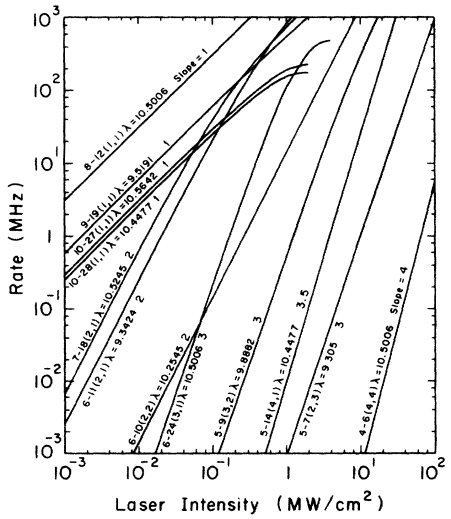

FIG. 7. Estimated higher-order CO_2 laser multiphoton ionization rates for electrically polarized hydrogen atoms with n as low as 4. The curves are labeled according to quantum numbers for the initial and intermediate states, along with the partial orders (k_1,k_2) for the bound-bound and bound-continuum multiphoton transitions, the resonant wavelength selected for each calculation, and the slope p of each rate curve. Every case with $n>5$ exhibits bottleneck behavior from either the bound-bound or the bound-continuum step, i.e., p is either k_1 or k_2.

This two-state result is nonperturbative in that portion of the photon absorption arising from the oscillating Stark effect that is nonzero for states with permanent electric dipole moments. It reduces to the leading term of perturbation theory,[30,31] when the Bessel function is approximated by its leading term. A more rigorous discussion[33] of the photon absorption associated with the permanent dipole moment indicates that the Bessel function in Eq. (17) should be replaced by

$$\frac{2\alpha\omega}{(z_{nn}-z_{n'n'})F}J_{\alpha}((z_{nn}-z_{n'n'})F/\omega), \tag{18}$$

which to within the sign has the same low field-strength limit. For the present purposes of order-of-magnitude estimates of multiphoton rates, either Eq. (17) or (18) could be used. We see from Eq. (17) that the dominant strong-field two-state multiphoton modifications of Ω_R and of R_{2c} are just to include the appropriate Bessel function factors of Eq. (18). Figure 7 shows some on-resonance estimates obtained this way for multiphoton ionization by CO_2-laser fields of electrically polarized hydrogen atoms with n between 4 and 10, obtained using both diagonal and off-diagonal matrix elements for the extreme Stark bound states[31] ignoring diagonal matrix elements of continuum states, and using the formula[18] for the n scaling of the p-state photoionization cross section describing the off-diagonal coupling between intermediate and continuum states. Although these first estimates may be in considerable error, they do further support the conclusions of our experiments that higher laser intensities are required for the multiphoton ionization of states other than $n=8$. A third-order perturbative calculation at one wavelength for substate-averaged $n=7$ atoms also supports this conclusion.[1] Precision experiments using electrically polarized hydrogenic atoms that would test theoretical predictions such as those shown in Fig. 7 appear to be difficult but possible.

ACKNOWLEDGMENT

The authors thank the National Science Foundation for its support.

[1]Y. Justum and A. Maquet, J. Phys. B **10**, L287 (1977).
[2]I. Ya. Berson, Zh. Eksp. Teor. Fiz. **83**, 1276 (1982) [Sov. Phys.—JETP **56**, 731 (1982)].
[3]P. Lambropoulos, Phys. Rev. A **9**, 1992 (1974).
[4]J. H. Eberly, Phys. Rev. Lett. **42**, 1049 (1979).
[5]L. A. Lompre, G. Mainfray, C. Manus, and J. P. Marinier, J. Phys. B **14**, 4307 (1981).
[6]P. Zoller, J. Phys. B **15**, 2911 (1982).
[7]P. Pignolet, B. Dubreuil, and A. Catherinot, J. Phys. B **15**, 2307 (1982).
[8]A. Maquet, Phys. Lett. **48A**, 199 (1974).
[9]B. Dubreuil, Phys. Lett. **51A**, 377 (1975).
[10]B. A. Zon. Opt. Spectrosc. **42**, 6 (1977).
[11]T. C. Landgraf, J. R. Leite, N. S. Almeida, C. A. S. Lima, and L. C. M. Miranda, Phys. Lett. **92A**, 131 (1982).
[12]J. E. Bayfield, Rev. Sci. Instrum. **47**, 1450 (1976).
[13]J. E. Bayfield, G. A. Khayrallah, and P. M. Koch, Phys. Rev. A **9**, 209 (1974).
[14]R. H. MacFarland, Phys. Rev. A **2**, 1795 (1970).
[15]D. S. Bailey, J. R. Hiskes, and A. C. Riviere, Nucl. Fusion **5**, 41 (1965).
[16]U. P. Oppenheim and M. Naftaly, Appl. Opt. **23**, 661 (1984).
[17]J. R. Hiskes and C. B. Tarter, Lawrence Livermore Radiation Laboratory, Report No. UCRL-7088, 1964 (unpublished); J. R. Hiskes, C. B. Tarter, and D. A. Moody, Phys. Rev. **133**, A424 (1964).
[18]W. J. Karzas and R. Latter, Astrophys. J. Suppl. **6**, 167 (1961).
[19]F. James and M. Roos, Comput. Phys. Commun. **10**, 343 (1975).
[20]J. E. Bayfield and L. A. Pinnaduwage, J. Phys. B **18**, L49 (1985).
[21]J. E. Bayfield and L. A. Pinnaduwage, Phys. Rev. Lett. **54**, 313 (1985); J. N. Bardsley, B. Sundaram, L. Pinnaduwage, and J. E. Bayfield, Phys. Rev. Lett. **56**, 1007 (1986).
[22]S. L. Shin, F. Yergeau, and P. Lavigne, J. Phys. B **18**, L213 (1985).
[23]R. J. Dewhurst, G. J. Pert, and A. M. Scott, J. Phys. B **13**, 2759 (1980).
[24]J. E. Bayfield, Phys. Rep. **51**, 317 (1979).
[25]G. Casati, B. V. Chirikov, and D. L. Shepelyansky, Phys. Rev. Lett. **53**, 2525 (1984).
[26]P. B. Corkum, IEEE J. Quantum Electronics **QE-21**, 216 (1985).
[27]P. W. Milonni and J. H. Eberly, J. Chem. Phys. **68**, 1602 (1978).
[28]D. Blochinzew, Phys. Z. Sowjetunion **4**, 501 (1933).
[29]J. E. Bayfield, L. D. Gardner, Y. Z. Gulkok, and S. D. Sharma, Phys. Rev. A **24**, 138 (1981).
[30]W. J. Meath and E. A. Power, J. Phys. B **17**, 763 (1984).
[31]J. N. Bardsley and B. Sundaram, Phys. Rev. A **32**, 689 (1985).
[32]T. S. Luk, H. Pummer, K. Boyer, M. Shahidi, H. Egger, and C. K. Rhodes, Phys. Rev. Lett. **51**, 110 (1983).
[33]G. F. Thomas, Phys. Rev. A **33**, 1033 (1986).